LETTER

doi:10.1038/nature10331

Protection of repetitive DNA borders from self-induced meiotic instability

Gerben Vader[1]*, Hannah G. Blitzblau[1]*, Mihoko A. Tame[1], Jill E. Falk[1]†, Lisa Curtin[1,2] & Andreas Hochwagen[1]†

DNA double strand breaks (DSBs) in repetitive sequences are a potent source of genomic instability, owing to the possibility of non-allelic homologous recombination (NAHR). Repetitive sequences are especially at risk during meiosis, when numerous programmed DSBs are introduced into the genome to initiate meiotic recombination[1]. In the repetitive ribosomal DNA (rDNA) array of the budding yeast *Saccharomyces cerevisiae*, meiotic DSB formation is prevented in part through Sir2-dependent heterochromatin formation[2,3]. Here we show that the edges of the rDNA array are exceptionally susceptible to meiotic DSBs, revealing an inherent heterogeneity in the rDNA array. We find that this localized DSB susceptibility necessitates a border-specific protection system consisting of the meiotic ATPase Pch2 and the origin recognition complex subunit Orc1. Upon disruption of these factors, DSB formation and recombination increased specifically in the outermost rDNA repeats, leading to NAHR and rDNA instability. Notably, the Sir2-dependent heterochromatin of the rDNA itself was responsible for the induction of DSBs at the rDNA borders in *pch2*Δ cells. Thus, although the activity of Sir2 globally prevents meiotic DSBs in the rDNA, it creates a highly permissive environment for DSB formation at the junctions between heterochromatin and euchromatin. Heterochromatinized repetitive DNA arrays are abundant in most eukaryotic genomes. Our data define the borders of such chromatin domains as distinct high-risk regions for meiotic NAHR, the protection of which may be a universal requirement to prevent meiotic genome rearrangements that are associated with genomic diseases and birth defects.

To understand better the mechanisms that protect repetitive DNA from meiotic NAHR, we analysed the single tandem rDNA array of budding yeast. Meiotic DSB formation and recombination in the rDNA are repressed by the histone deacetylase Sir2 (refs 2, 3). Additionally, Pch2, a widely conserved meiosis-specific ATPase, suppresses meiotic recombination in the rDNA by an unknown mechanism[4,5]. We used clamped-homogenous electric field (CHEF) electrophoresis and Southern blotting of excised rDNA arrays to address whether Pch2 regulates meiotic DSB formation in the rDNA. Consistent with previous results[2,3], the level of full-length rDNA arrays that remained 8 h after meiotic induction was significantly reduced in *sir2*Δ mutants compared to wild-type cells, indicating increased DSB formation (Fig. 1a and Supplementary Fig. 1a). By contrast, no such reduction occurred in *pch2*Δ mutants, although we observed a tenfold increase in crossover recombination across the rDNA array (Fig. 1a, b). Because small changes in array length would not be detectable by the CHEF gel assay, we wondered whether DSB formation in *pch2*Δ mutants occurred specifically in the outermost rDNA repeats. To test this possibility, we generated *pch2*Δ strains carrying a *URA3* insertion at defined positions in the rDNA array (Fig. 1c) and analysed the rDNA repeat units that directly flank these insertions by Southern blotting. We observed a strongly DSB-prone site in repeat 1 and weak DSB formation in repeat 3, whereas no DSB formation was detectable in repeat 10 of the approximately 100 rDNA repeats (Fig. 1d). Thus, *pch2*Δ cells undergo increased meiotic DSB formation predominantly in the outermost rDNA repeats.

To determine whether *PCH2* suppresses DSB formation only within the rDNA, or also in other regions of the genome, we first analysed a chromosomal fragment spanning the junction between single-copy DNA and rDNA in a *pch2*Δ mutant by Southern blotting. We observed additional, strong DSB formation in the adjacent single-copy sequences (Fig. 1e and Supplementary Fig. 1b), which were previously shown to have exceptionally low levels of meiotic DSBs in *PCH2* cells[6,7] (Fig. 1f). The observed break sites behaved similarly to known meiotic DSBs[8]; they were induced during meiosis in *dmc1*Δ and *DMC1* cells (Fig. 1d, e and Supplementary Fig. 1c), depended on the meiotic DSB machinery (Supplementary Fig. 1d)[9], promoted meiotic recombination (Supplementary Fig. 1e) and occurred in gene promoters (Fig. 1e and Supplementary Fig. 1b). Indeed, even the DSBs observed in repeat 1 mapped to the promoter of a gene (*TAR1*) that is encoded in every rDNA repeat[10] (Fig. 1e). Genome-wide analysis of DSBs[6] in *pch2*Δ cells showed that strong DSB induction occurred in 30–50-kilobase (kb) regions of single-copy sequence abutting both sides of the rDNA (Fig. 1f). Increased DSB formation was also observed close to other heterochromatic regions (telomeres and *HML*), whereas the DSB landscape elsewhere in the genome was not markedly altered (Supplementary Figs 1f, g, 2 and Supplementary Table 1). In contrast to *pch2*Δ mutants, the loss of *SIR2* did not lead to increased DSB formation adjacent to the rDNA array (Fig. 1f). Thus, Pch2 represses recombination in the rDNA at the level of DSB formation, but in a manner distinct from Sir2.

We investigated whether the increased DSB formation in the outermost rDNA repeats in *pch2*Δ mutants (Fig. 1d) resulted in a local increase in rDNA recombination. We measured recombination rates using flanking markers to the left and right of the rDNA together with a collection of single *URA3* insertions tiling inwards from the left side of the rDNA (Fig. 1c). Analysis of a *URA3* insertion in the centre of the rDNA (inserted next to repeat 49 of 99) indicated that recombination occurred in a symmetrical pattern. Notably, about 80% of the recombination events in the left half of the rDNA occurred within the first ten repeats from the left border (Fig. 1g and Supplementary Table 2), with about 30% taking place within repeat 1. Thus, there is a strong bias for recombination in the rDNA repeats very close to the array border.

Because recombination in repetitive DNA can lead to NAHR, we selected tetrads of *pch2*Δ mutants that had undergone recombination in the rDNA, and determined the resulting rDNA repeat number between the *URA3* insertion and the left rDNA boundary. In 70% ($n = 47$) of the tetrads investigated from different *URA3* integrants, we detected changes in repeat number, ranging from 1 to 19 repeats (Fig. 1i, j and Supplementary Table 2), demonstrating that rDNA crossovers in *pch2*Δ cells are frequently associated with NAHR.

[1]Whitehead Institute for Biomedical Research, 9 Cambridge Center, Cambridge, Massachusetts 02142, USA. [2]Somerville High School, Somerville, Massachusetts 02143, USA. †Present addresses: David H. Koch Institute for Integrative Cancer Research, Massachusetts Institute of Technology, Cambridge, Massachusetts 02139, USA (J.E.F.); Department of Biology, New York University, 100 Washington Square East, New York, New York 10003, USA (A.H.).
*These authors contributed equally to this work.

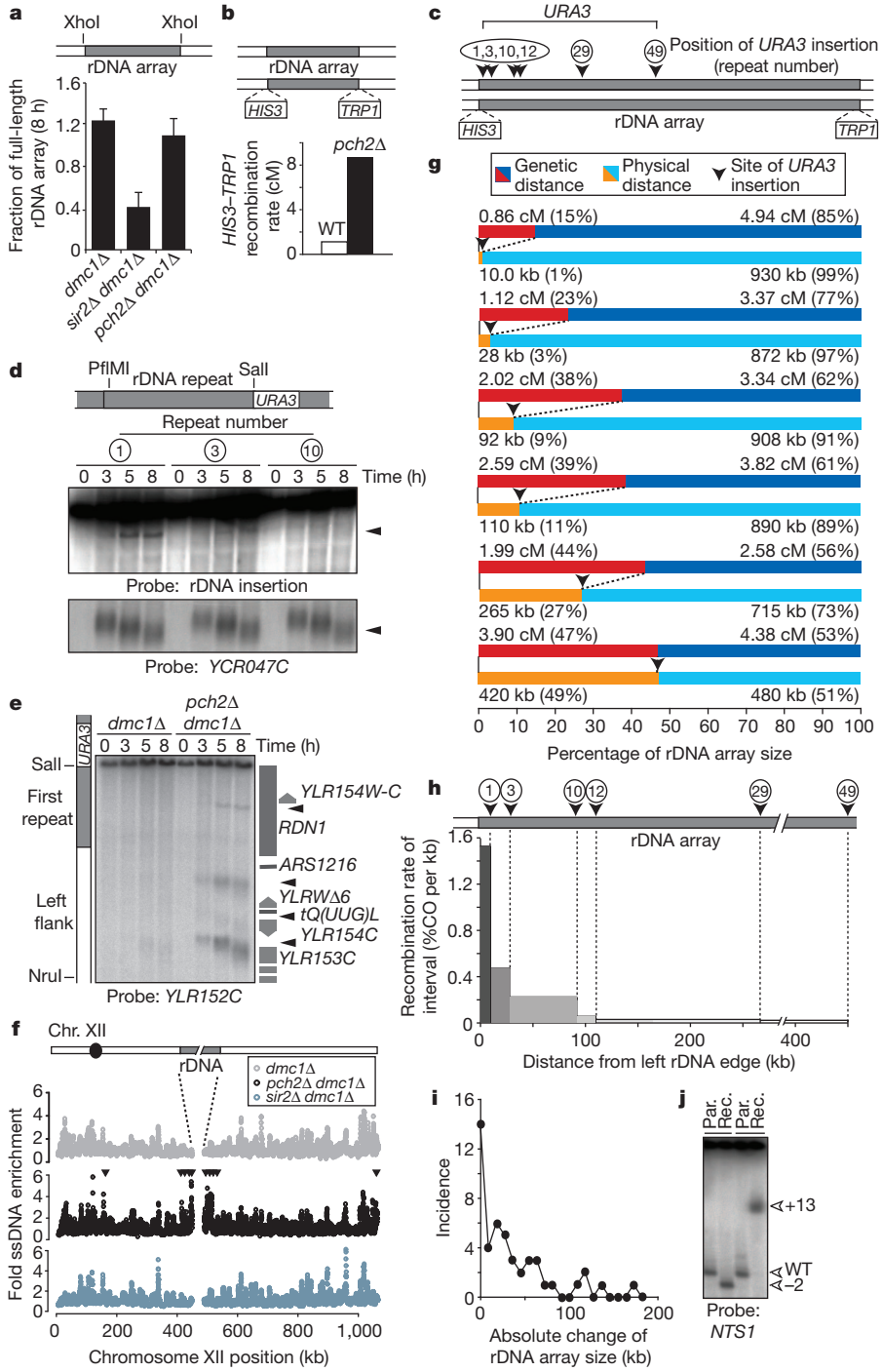

Figure 1 | Ribosomal-DNA-associated DSB formation and recombination. **a**, CHEF analysis of the rDNA of meiotic *dmc1*Δ (H5217), *sir2*Δ *dmc1*Δ (H2953) and *pch2*Δ *dmc1*Δ (H5216) cells. The schematic shows the analysed XhoI restriction fragment. A *dmc1*Δ mutation was used to prevent DSB repair. The mean (+ s.e.m.) of five experiments is shown. Significance was assessed by one-tailed Student's *t*-test: *dmc1*Δ versus *sir2*Δ *dmc1*Δ, *P* value = 0.00122; *dmc1*Δ versus *pch2*Δ *dmc1*Δ, *P* value = 0.254; *pch2*Δ *dmc1*Δ versus *sir2*Δ *dmc1*Δ, *P* value = 0.00216. **b**, Schematic of markers inserted in unique single-copy sequences within 500 base pairs (bp) of the rDNA, and crossover rates in wild-type (WT; H3026; $n = 467$) and *pch2*Δ (H3027; $n = 186$) cells. **c**, Schematic indicating marker locations in the rDNA used in **d** and **g**. *URA3* markers were inserted in the *NTS1/2* region of the indicated repeats. **d**, Southern blot for restriction fragments containing the indicated insert-associated rDNA repeat units from *pch2*Δ *dmc1*Δ strains H5622 (repeat 1), H5636 (repeat 3) and H5706 (repeat 10). DNA was digested with PflMI and SalI and probed for the unique rDNA insertion. The *YCR047C* probe (on DNA digested with HindIII) was a positive control for DSB formation. **e**, Southern blot of the left rDNA flank, including the outermost rDNA repeat, in *dmc1*Δ (H5583) and *pch2*Δ *dmc1*Δ (H5622) cells (SalI and NruI digest; probe *YLR152C*). Positions of open reading frames are shown schematically alongside the Southern blot. **f**, Enrichment profile of ssDNA in chromosome XII in *dmc1*Δ (H118, light grey), *pch2*Δ *dmc1*Δ (H2629, black) and *sir2*Δ *dmc1*Δ (H2953, dark grey) cells. Arrowheads indicate >twofold increased DSB formation in *pch2*Δ *dmc1*Δ compared to *dmc1*Δ cells. **g**, Tetrad analysis of *pch2*Δ *URA3*-rDNA-insertion strains H4611 (repeat 1), H4613 (repeat 3), H3823 (repeat 10), H4612 (repeat 12), H3820 (repeat 29) and H3821 (repeat 49; Supplementary Table 2). Recombination rates between *URA3* and rDNA-flanking markers are shown in relation to the physical *URA3* positions in the rDNA. **h**, Relative contribution of each measured interval indicated in **g** to total rDNA recombination (percentage of crossovers (CO) per kb of interval). **i**, Incidence of changes in rDNA repeat number between the *URA3* insertion and the rDNA boundary in *pch2*Δ tetrads that had undergone crossover recombination. **j**, CHEF analysis of two tetrads that have undergone unequal recombination with parental controls. DNA was digested with XhoI and probed with *NTS1*. Par., parental controls; Rec., recombinants.

However, the prevalence of allelic recombinants (30%) and the fact that changes in repeat number encompassed less than 20% of the approximately 100–110 rDNA repeats in our strains indicate that the homology search for DSB repair in the outermost rDNA repeats in *pch2*Δ cells is restricted to close neighbours. Notably, the distribution of changes in repeat number closely matched the pattern of crossover events (Fig. 1h, i). This congruence indicates that the spread in the crossover distribution (Fig. 1g, h) can largely be accounted for by non-allelic exchanges between rDNA repeats originating from DSBs in the outermost repeats of the array. Finally, although rDNA exchanges occurred at a much lower frequency in wild-type cells, they were also associated with NAHR (Supplementary Table 2), indicating that Pch2 primarily acts to prevent NAHR by suppressing DSB formation. These results establish the rDNA borders as high-risk regions for meiotic NAHR.

To determine how Pch2 suppresses DSB formation near the rDNA, we measured the chromosome association of DSB-related factors at the time of DSB formation. The three essential DSB factors[11,12] that we were able to analyse by chromatin immunoprecipitation (ChIP), Rec114, Mer2 and Mre11, were specifically enriched near the rDNA and *HML* in *pch2*Δ cells, mirroring the changes in DSB formation (Fig. 2 and Supplementary Fig. 3). We then investigated whether the regional exclusion of DSB factors could be explained by local depletion of the DSB-promoting chromosome-axis protein Hop1, the cytological distribution of which is affected by Pch2 (refs 4, 13). Although Hop1 binding was slightly increased near the rDNA and *HML* in *pch2*Δ cells, it was abundant even in wild-type cells, indicating that Pch2 does not regulate the initial chromosomal recruitment of Hop1. Rather, the differences in Hop1 binding that we observed might reflect an effect of Pch2 on chromosome structure[13]. Finally, although DSBs are enriched in promoters containing histone H3 lysine 4 trimethylation (H3K4me3)[14], we saw no difference in the genome-wide levels of this modification with or without Pch2 (Fig. 2c and Supplementary Figs 3d and 4), indicating that Pch2 does not influence this chromatin modification. These findings indicate that Pch2 specifically blocks the stable recruitment of DSB factors to prevent local DSB formation.

We sought to identify proteins that collaborate with Pch2 in preventing rDNA-proximal DSBs. A yeast two-hybrid screen isolated a fragment of the Orc1 protein, containing its ATPase domain, as a Pch2 interactor (Fig. 3a). This interaction was confirmed by co-immunoprecipitation (Fig. 3b and Supplementary Fig. 5a). Orc1 is a component of the conserved origin recognition complex that has several important chromosomal functions, including the loading of the replicative helicase[15]. Impairing Orc1 protein levels by a temperature-sensitive *orc1-161* mutation[16] (Supplementary Fig. 5b) triggered DSB formation in the rDNA flanking regions, similarly to the loss of *PCH2* (Fig. 3c, d). DSB formation near the rDNA occurred even at a temperature (23 °C) that is permissive for pre-meiotic DNA replication and spore viability (Fig. 3c–e and Supplementary Fig. 5c, d). Similarly, we saw increased DSB levels near the rDNA in an *orc1* mutant lacking the N-terminal bromo-adjacent homology (BAH) domain that is required for the chromatin-silencing function of Orc1 (ref. 17), but is dispensable for DNA replication (Fig. 3f and Supplementary Fig. 5e, f). These data indicate that the regulatory roles of Orc1 in DSB formation and bulk DNA replication are separable, although we cannot rule out that the analysed *orc1* mutations affect rDNA replication locally. During meiosis, Pch2 concentrates in the nucleolus, the organelle assembled on the rDNA array[4]. In *orc1-161* cells, the recruitment of Pch2 to the nucleolus was impaired, despite normal levels of cellular Pch2 (Fig. 3g, h). Both Pch2 and Orc1 belong to the AAA^+ family of ATPases that often function as multimeric complexes[18], and we found that the ATPase activity of Pch2 was required to prevent rDNA-proximal DSBs (Supplementary Fig. 5g). These data define a role for Orc1 in the nucleolar recruitment and possible activation of Pch2 to prevent local DSB formation.

To find out whether the specific DSB activity at the rDNA borders in *pch2*Δ mutants was linked to the presence of the rDNA itself, we deleted the rDNA array from its genomic location. In these strains, loss of *PCH2* no longer allowed DSB formation in the flanking regions (Figs 4a, b), demonstrating an intrinsic DSB-promoting activity in the rDNA. To investigate whether the rDNA was sufficient to promote DSB formation, we created a translocation between chromosomes II and XII that exchanged the rDNA-distal portion of chromosome XII with a portion of chromosome II (Fig. 4c). In these strains, DSB levels were no longer increased in the former right flank of the rDNA (now flanked by chromosome II sequences; Fig. 4d), but notably, increased DSB formation was observed on the chromosome II sequences that, after translocation, were flanking the rDNA (Fig. 4e). Thus, in the absence of *PCH2*, the rDNA is necessary and sufficient to promote DSB formation.

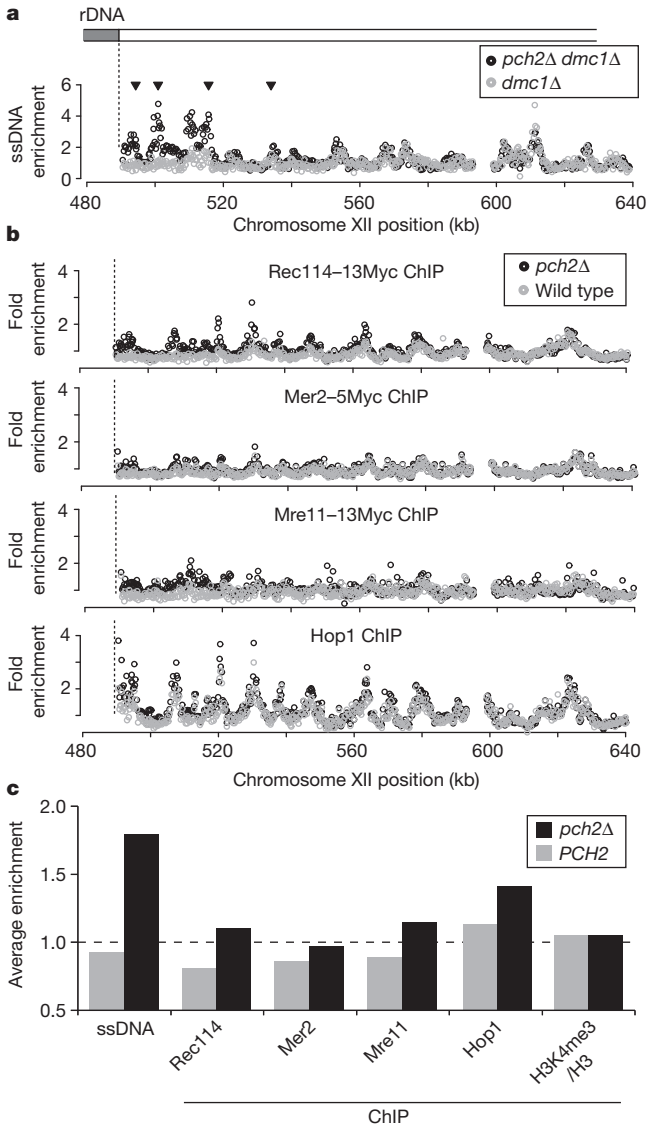

Figure 2 | Association of the meiotic DSB machinery near the rDNA. **a**, Enrichment of ssDNA in a region flanking the right border of the rDNA on chromosome XII (*Saccharomyces* genome database (SGD) coordinates) in *dmc1*Δ (H118, grey) and *pch2*Δ *dmc1*Δ (H2629, black) cells. Arrowheads indicate >twofold increased DSB formation in *pch2*Δ *dmc1*Δ compared to *dmc1*Δ cells. **b**, ChIP-chip analysis in same region as in **a**, for the proteins Rec114–13Myc (first panel; wild type (H4890), *pch2*Δ (H4893)), Mer2–5Myc (second panel; wild type (H5917), *pch2*Δ (H5916)), Mre11–13Myc (third panel; wild type (H5547), *pch2*Δ (H5947)) and Hop1 (fourth panel; wild type (H119), *pch2*Δ (H2817)), in wild-type (grey) and *pch2*Δ (black) cells. **c**, Average enrichment for the different *PCH2* and *pch2*Δ ssDNA and ChIP data sets (see **a**, **b** and Supplementary Fig. 4) within the 50 kb flanking the right rDNA border (see Methods for genomic coordinates). The genome-wide average is indicated by the dotted line.

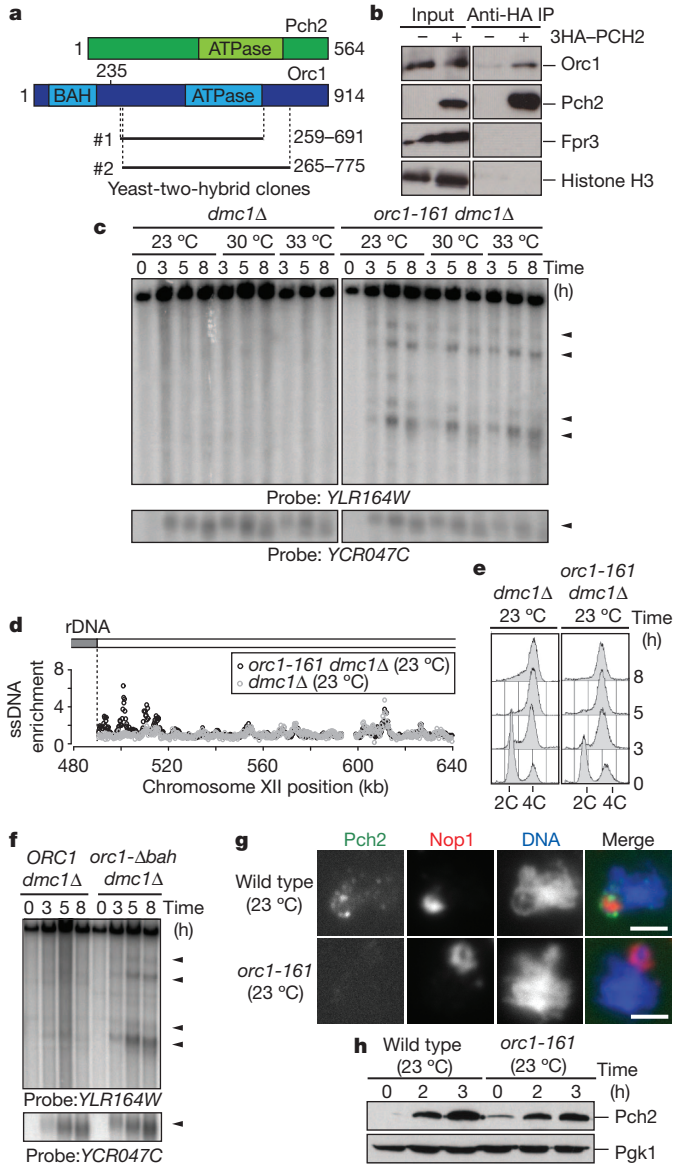

Figure 3 | Orc1 and Pch2 collaborate to suppress DSB formation. **a**, Schematic of Pch2 and Orc1 proteins, indicating Orc1 clones identified by yeast two-hybrid screen. **b**, Co-immunoprecipitation (IP) between haemagglutinin-tagged Pch2 (3HA–Pch2) and Orc1 in wild-type (H119) and *3HA–PCH2* (H3463) cells. Fpr3 and histone H3 are controls for the nucleolar and chromosomal fractions, respectively. **c**, Southern blots of the right rDNA flank and *YCR047C* in meiotic *dmc1*Δ (H118) and *orc1-161 dmc1*Δ (H4952) cells, grown at the indicated temperatures. Arrowheads indicate broken DNA fragments. **d**, Profiles of ssDNA in the region flanking the right rDNA border in *orc1-161 dmc1*Δ (H5137, black) and *dmc1*Δ (H118, grey) cells, grown at 23 °C. **e**, DNA-content analysis of meiotic *dmc1*Δ (H118) and *orc1-161 dmc1*Δ (H5137) cells grown at 23 °C. 2C and 4C refer to unreplicated and replicated diploid DNA contents, respectively. **f**, Southern blots of the right rDNA flank and *YCR047C* in *ORC1 dmc1*Δ (H5838) and *orc1-Δbah dmc1*Δ (H5865) cells. **g**, Immunofluorescence of chromosome spreads stained for Pch2 (HA, green), Nop1 (nucleolar marker, red) and DNA (blue) in *3HA–PCH2* (H3463) and *3HA–PCH2 orc1-161* (H5033) cells at 3 h after meiotic induction at 23 °C. Scale bar, 2 μm. **h**, Western blot analysis showing Pch2 (HA) expression in *3HA–PCH2* (H3463) and *3HA–PCH2 orc1-161* (H5033) cells. Pgk1 is used as loading control.

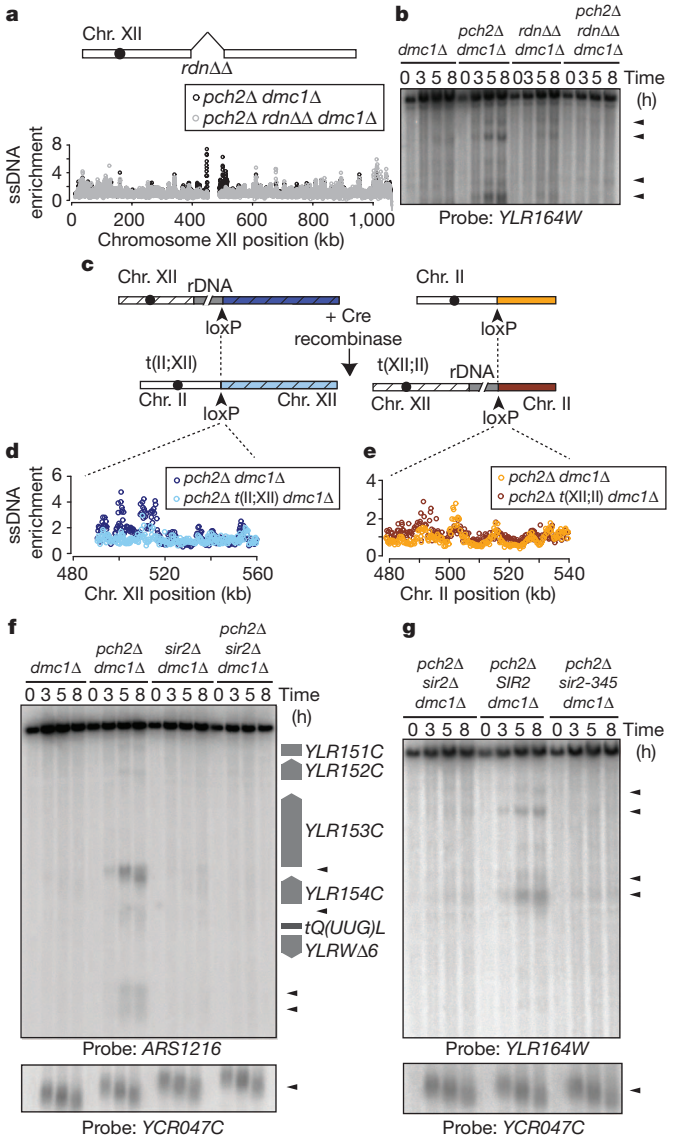

Figure 4 | Ribosomal-DNA chromatin promotes DSB formation. **a**, Schematic of the rDNA deletion strain (*rdn*ΔΔ) and ssDNA profiles of the region flanking the right rDNA border in *pch2*Δ *dmc1*Δ (H2629, black) and *pch2*Δ *rdn*ΔΔ *dmc1*Δ (H4737, grey) cells. **b**, Southern blot analysis of the right rDNA flank in *dmc1*Δ (H118), *pch2*Δ *dmc1*Δ (H2629), *rdn*ΔΔ *dmc1*Δ (H4736) and *pch2*Δ *rdn*ΔΔ *dmc1*Δ (H4737) cells. Arrowheads indicate broken DNA fragments. **c**, Strategy used to generate chromosomal translocations between chromosomes XII and II. **d**, **e**, Profiles of ssDNA in strains containing the XII;II translocation. In **d**, the depicted region is next to the rDNA in *pch2*Δ *dmc1*Δ (H2629) cells (dark blue) and next to the left arm of chromosome II in *pch2*Δ t(II;XII) *dmc1*Δ (H4798) cells (light blue). In **e**, the depicted region is located on chromosome II in *pch2*Δ *dmc1*Δ cells (orange) and next to rDNA in *pch2*Δ t(XII;II) *dmc1*Δ cells (dark red). **f**, Southern blot of the left rDNA flank (HindIII digest; *ARS1216* probe) and of *YCR047C* in *dmc1*Δ (H118), *pch2*Δ *dmc1*Δ (H2629), *sir2*Δ *dmc1*Δ (H2953) and *pch2*Δ *sir2*Δ *dmc1*Δ (H3038) cells. Positions of open reading frames are shown schematically alongside the Southern blot. **g**, Southern blot of the right rDNA flank and *YCR047C* in *pch2*Δ *sir2*Δ *dmc1Δ* (H3262), *pch2*Δ *sir2*Δ *dmc1*Δ *leu2::SIR2* (H3261) and *pch2*Δ *sir2*Δ *dmc1*Δ *leu2::sir2-345* (H3282) cells. Arrowheads indicate broken DNA fragments.

The rDNA is assembled into specialized, Sir2-dependent chromatin, and we asked how this chromatin state influenced DSB formation at the rDNA boundaries. Notably, loss of Sir2 protein or loss of its deacetylase activity[19] largely eliminated DSB formation in the rDNA flanking regions in *pch2*Δ mutants (Fig. 4f, g). Thus, although Sir2-dependent heterochromatin suppresses meiotic DSBs within the rDNA array (refs 2, 3 and Fig. 1a), it has a profound DSB-promoting effect on the rDNA borders that is counteracted by Pch2 and Orc1. It is also notable that Sir2 itself localizes Pch2 to the nucleolus[4], reflecting an elegant coupling mechanism that maintains meiotic stability across the entire rDNA. The double dependence of Pch2 on Sir2 and Orc1

may promote Pch2 enrichment at the nucleolus, analogous to the bimodal recruitment mechanisms that restrict localization of Aurora B and shugoshin to centromeres[20].

Although repeat-associated chromatin marks differ substantially between organisms and even among individual loci[21], the assembly of heterochromatin on repetitive DNA arrays is a common strategy to protect the genome against destabilization caused by errors in meiotic recombination[1]. Our results establish borders between heterochromatin and euchromatin as potential high-risk regions for meiotic DSB formation and NAHR, and reveal the existence of a secondary border-specific system that shields against these events. Buffer zones like those established by Pch2 and Orc1 may need to be broad, because even DSBs adjacent to repetitive DNA can trigger NAHR[22]. Given the prominent presence of repetitive DNA arrays in genomes ranging from yeast to man[1], we propose that mechanisms that limit DSB activity around repetitive DNA might be a widespread phenomenon.

METHODS SUMMARY

Yeast strains were of the SK1 background and are listed in Supplementary Table 3. Analysis of single-stranded DNA profiles and ChIP-chip analysis were performed as previously described[6,23]. These and other standard techniques used are detailed in the Methods.

Full Methods and any associated references are available in the online version of the paper at www.nature.com/nature.

Received 18 January; accepted 24 June 2011.
Published online 7 August 2011.

1. Sasaki, M., Lange, J. & Keeney, S. Genome destabilization by homologous recombination in the germ line. *Nature Rev. Mol. Cell Biol.* **11,** 182–195 (2010).
2. Gottlieb, S. & Esposito, R. E. A new role for a yeast transcriptional silencer gene, *SIR2*, in regulation of recombination in ribosomal DNA. *Cell* **56,** 771–776 (1989).
3. Mieczkowski, P. A. *et al.* Loss of a histone deacetylase dramatically alters the genomic distribution of Spo11p-catalyzed DNA breaks in *Saccharomyces cerevisiae*. *Proc. Natl Acad. Sci. USA* **104,** 3955–3960 (2007).
4. San-Segundo, P. A. & Roeder, G. S. Pch2 links chromatin silencing to meiotic checkpoint control. *Cell* **97,** 313–324 (1999).
5. Wu, H. Y. & Burgess, S. M. Two distinct surveillance mechanisms monitor meiotic chromosome metabolism in budding yeast. *Curr. Biol.* **16,** 2473–2479 (2006).
6. Blitzblau, H. G. *et al.* Mapping of meiotic single-stranded DNA reveals double-stranded-break hotspots near centromeres and telomeres. *Curr. Biol.* **17,** 2003–2012 (2007).
7. Gerton, J. L. *et al.* Inaugural article: global mapping of meiotic recombination hotspots and coldspots in the yeast *Saccharomyces cerevisiae*. *Proc. Natl Acad. Sci. USA* **97,** 11383–11390 (2000).
8. Petes, T. D. Meiotic recombination hot spots and cold spots. *Nature Rev. Genet.* **2,** 360–369 (2001).
9. Keeney, S. Mechanism and control of meiotic recombination initiation. *Curr. Top. Dev. Biol.* **52,** 1–53 (2001).
10. Coelho, P. S. *et al.* A novel mitochondrial protein, Tar1p, is encoded on the antisense strand of the nuclear *25S* rDNA. *Genes Dev.* **16,** 2755–2760 (2002).
11. Arora, C., Kee, K., Maleki, S. & Keeney, S. Antiviral protein Ski8 is a direct partner of Spo11 in meiotic DNA break formation, independent of its cytoplasmic role in RNA metabolism. *Mol. Cell* **13,** 549–559 (2004).
12. Keeney, S. & Neale, M. J. Initiation of meiotic recombination by formation of DNA double-strand breaks: mechanism and regulation. *Biochem. Soc. Trans.* **34,** 523–525 (2006).
13. Borner, G. V., Barot, A. & Kleckner, N. Yeast Pch2 promotes domainal axis organization, timely recombination progression, and arrest of defective recombinosomes during meiosis. *Proc. Natl Acad. Sci. USA* **105,** 3327–3332 (2008).
14. Borde, V. *et al.* Histone H3 lysine 4 trimethylation marks meiotic recombination initiation sites. *EMBO J.* **28,** 99–111 (2009).
15. Bell, S. P. The origin recognition complex: from simple origins to complex functions. *Genes Dev.* **16,** 659–672 (2002).
16. Gibson, D. G., Bell, S. P. & Aparicio, O. M. Cell cycle execution point analysis of ORC function and characterization of the checkpoint response to ORC inactivation in *Saccharomyces cerevisiae*. *Genes Cells* **11,** 557–573 (2006).
17. Bell, S. P. *et al.* The multidomain structure of Orc1p reveals similarity to regulators of DNA replication and transcriptional silencing. *Cell* **83,** 563–568 (1995).
18. Hanson, P. I. & Whiteheart, S. W. AAA+ proteins: have engine, will work. *Nature Rev. Mol. Cell Biol.* **6,** 519–529 (2005).
19. Imai, S., Armstrong, C. M., Kaeberlein, M. & Guarente, L. Transcriptional silencing and longevity protein Sir2 is an NAD-dependent histone deacetylase. *Nature* **403,** 795–800 (2000).
20. Vader, G. & Lens, S. M. Chromosome segregation: taking the passenger seat. *Curr. Biol.* **20,** R879–R881 (2010).
21. Moazed, D. Common themes in mechanisms of gene silencing. *Mol. Cell* **8,** 489–498 (2001).
22. Hoang, M. L. *et al.* Competitive repair by naturally dispersed repetitive DNA during non-allelic homologous recombination. *PLoS Genet.* **6,** e1001228 (2010).
23. Aparicio, O. M., Weinstein, D. M. & Bell, S. P. Components and dynamics of DNA replication complexes in *S. cerevisiae*: redistribution of MCM proteins and Cdc45p during S phase. *Cell* **91,** 59–69 (1997).

Supplementary Information is linked to the online version of the paper at www.nature.com/nature.

Acknowledgements We thank S. P. Bell, A. Shinohara, N. Hunter, N. Hollingsworth and F. Klein for sharing reagents and data. We thank I. Cheeseman, M. Gehring and V. Subramanian for discussions and critical reading of the manuscript. This work was supported by NIH grant GM088248 to A.H. and by fellowships from the Netherlands Organisation for Scientific Research (NWO Rubicon-825.08.009 and NWO VENI-016.111.004) to G.V.; L.C. was supported by an HHMI Institutional Undergraduate Education Grant to MIT (grant 52005879).

Author Contributions G.V., H.G.B. and A.H. designed and performed experiments and analysed the data. M.A.T. performed the yeast two-hybrid analysis. J.E.F., L.C. and A.H. performed recombination mapping. G.V., H.G.B. and A.H. wrote the paper.

Author Information All data sets in this publication are available in the NCBI Gene Expression Omnibus (http://www.ncbi.nlm.nih.gov/geo/), accession number GSE30073. Reprints and permissions information is available at www.nature.com/reprints. The authors declare no competing financial interests. Readers are welcome to comment on the online version of this article at www.nature.com/nature. Correspondence and requests for materials should be addressed to A.H. (andi@nyu.edu).

METHODS

Yeast strains and two-hybrid analysis. All yeast strains used in this study were constructed in the SK1 background and are listed in Supplementary Table 3. Epitope tags and gene disruptions were introduced by standard PCR-based transformation. The *orc1-Δbah* mutant was generated using a plasmid encoding a truncated version of Orc1 (amino acids 235–914; pSPB1.48, gift from S. P. Bell[24]). To create *URA3* insertions in the rDNA, cells were transformed with a pRS306-NTS1/2 plasmid linearized with SphI (this plasmid contains a 2341-bp fragment harbouring the intergenic rDNA sequences, *NTS1* and *NTS2*, ligated into the BamHI and EcoRI sites of pRS306). Insertion sites in the rDNA were mapped by CHEF gel analysis using a unique XhoI site in the inserted sequence (XhoI does not cut in the rDNA), and suitable clones were selected for further analysis. SK1 strains lacking the rDNA array were generated as described in ref. 25. Briefly, cells were transformed with a very high-copy rDNA plasmid (*pRDN-hyg::URA3::leu2-8*) carrying a recessive point mutation that confers resistance to hygromycin[26]. After selection on hygromycin, a clone was selected that had lost all but three repeats of the rDNA array through spontaneous deletion, as determined by CHEF gel analysis. The remaining rDNA copies were subsequently deleted by conventional gene disruption using a *HIS3* deletion cassette. Complete deletion of the rDNA array was confirmed by Southern blotting. Chromosomal translocations between chromosomes XII and II were generated essentially as previously described[27]. Briefly, plasmids containing a promoter-less *ADE2* gene adjacent to a *loxP* site (*loxP-ADE2::natMX4*) and a *GPD* promoter (*pGPD*) with an adjacent *loxP* site (*pGPD-loxP::hphMX4*; both plasmids were gifts from N. Hunter) were integrated at *YLR162W-A* and *LYS2*, respectively. After induction of Cre recombinase from a pGAL-Cre plasmid (N. Hunter), cells were selected that had undergone translocation between *LYS2* (chromosome II) and *YLR162W-A* (chromosome XII). Translocation was confirmed by Southern blot analysis. To identify interactors of Pch2 by two-hybrid screen, full-length *PCH2* was amplified from genomic DNA and the intron was removed by site-directed mutagenesis. The Pch2 coding sequence was then cloned into pGBDU-C1, and the resulting bait plasmid was used to screen libraries in all three reading frames[28].

Synchronous meiosis. Cells were grown for 24 h in yeast peptone dextrose (YPD) at 23 °C then diluted in BYTA medium (1% yeast extract, 2% tryptone, 1% potassium acetate, 50 mM potassium phthalate) to a optical density at 600 nm (OD_{600}) of 0.3 (OD_{600} = 0.5 for *orc1-161*, *rdnΔΔ* and XII;II translocation strains), and grown for 16 h at 30 °C (or for 18 h at 23 °C in the case of temperature-sensitive strains). After two washes in water, cells were diluted into SPO medium (0.3% potassium acetate) at OD_{600} = 1.9 and incubated at 30 °C unless otherwise stated.

Isolation of ssDNA. For ssDNA analysis[29,30], about 10^9 cells were fixed in 70% ethanol at −20 °C at 0 h and 5 h after induction of meiosis. After spheroplasting in sorbitol buffer (1 M sorbitol, 1% β-mercaptoethanol, 0.2 mg ml^{-1} zymolyase, and 0.1 M EDTA, pH 7.4), cells were lysed in NDS buffer (0.6% SDS, 300 mM EDTA, 10 mM Tris-HCl, pH 9.5). After treatment with proteinase K (0.25 mg ml^{-1}) and RNase A, the DNA was digested with EcoRI and ssDNA was then enriched by adsorption to BND-cellulose and eluted using 1.8% caffeine. This enriched ssDNA was subsequently used for microarray analysis. For this, 1.5 μg of the respective 0-h and 5-h ssDNA samples was labelled with Cy3-dUTP or Cy5-dUTP (GE Healthcare) by random priming without denaturation using 4 μg of random primer (Integrated DNA Technologies) and 10 units of Klenow (New England Biolabs).

Western blotting and immunoprecipitation. For western blotting, 5 ml of meiotic cells were harvested at the indicated time points and resuspended in 5% trichloroacetic acid. After incubation on ice for 10 min, samples were washed in acetone and dried overnight. Samples were lysed by bead beating in a FastPrep FP120 (Thermo Scientific) in TE lysis buffer (10 mM Tris (pH 7.5), 1 mM EDTA, 2.75 mM dithiothreitol). SDS loading buffer (3×) was added and the pH of the sample was adjusted to neutral by addition of 1 M Tris (pH 8.0). Samples were separated by standard polyacrylamide gel electrophoresis. The following antibodies were used: anti-ORC (1108, 1:1,000, gift from S. P. Bell), anti-Fpr3 (1:1,000, gift from J. Thorner), anti-HA (3F10, 1:1,000, Roche), anti-Pgk1 (1:1,000, Invitrogen) and anti-histone H3 (1:1,000, Abcam). For immunoprecipitations, 50 ml of meiotic cells were harvested 3 h after induction of meiosis. Cells were diluted in 2× lysis buffer (20 mM HEPES (pH 7.5), 4 mM $MgCl_2$, 0.6 M glutamic acid, 0.32 M sorbitol, 4% glycerol, 0.5% Triton X-100) containing protease inhibitors, and lysed by bead beating. Extracts were sonicated and cleared by centrifugation. After removal of one tenth of the extract for an input sample, extracts were immunoprecipitated with 2 μl anti-HA (3F10, Roche) for 3HA–Pch2, 2 μl anti-ORC (1108) and 2 μl anti-Fpr3, in combination with 20 μl of a 50% slurry of GammaBind-Sepharose beads (GE Healthcare) for 16 h at 4 °C. After five washes in 1× lysis buffer, 1× SDS loading buffer was added to the beads, and samples were analysed by western blotting with the indicated antibodies.

Chromatin immunoprecipitation. Meiotic cells (25 ml) were harvested 3 h after induction of meiosis and fixed for 15 min in 1% formaldehyde. The formaldehyde was quenched by addition of 125 mM glycine. Samples were processed as previously described[23]. Before immunoprecipitation, one tenth of the sample was removed as input sample. The antibodies used for immunoprecipitation were: 2 μl anti-Myc (9E11, Abcam; for Rec114–13Myc, Mer2–5Myc and Mre11–13Myc), 2 μl anti-Hop1 (gift from N. Hollingsworth), 2 μl anti-histone-H3 (AB1791, Abcam) and 2 μl anti-H3K4me3 (AB8580, Abcam), in combination with 20 μl of a 50% slurry of GammaBind-Sepharose beads (GE Healthcare). Half of the ChIP sample and one tenth of the input were labelled with Cy3-dUTP or Cy5-dUTP (GE Healthcare) as described in the ssDNA protocol, with the difference that the DNA was denatured for 5 min at 95 °C before the extension reaction.

Microarray analysis. After removal of unincorporated dyes, Cy3- and Cy5-labelled samples were hybridized to custom 4 × 44K tiled genomic yeast microarrays (Agilent Technologies) for 16 h at 65 °C. Levels of Cy3 and Cy5 were calculated with the Agilent Feature Extractor CGH software. Background normalization, $\log_2$ ratios for each experiment and scale normalizations between experiments were calculated with the sma package in R (v2.1.0, http://www.r-project.org)[29,30]. Each data set is an average of two experiments. For comparison between isogenic wild-type and *pch2Δ* cells, data sets were scale-normalized. To analyse the distribution of H3K4me3, we normalized the enrichment to that of total histone H3 generated from the same extracts, by subtracting the $\log_2$ ratios. To measure the average ssDNA or ChIP enrichment in different chromosomal regions, the following SGD coordinates were analysed, on the basis of the positions of available array features:

50 kb right of the rDNA: XII, 490,531–540,530.
50 kb left of the rDNA: XII, 401,371–451,370.
Rest of chromosome XII: XII, 1–401,370 and 540,531–1,078,177.
First 100 kb of chromosome III: III, 1–100,000.
Rest of chromosome III: III, 100,001–316,620.
Chromosome VIII: VIII, 1–562,643.

Chromosome spreads and immunofluorescence. Meiotic cells were spread as described previously[31]. Cells were spheroplasted at 37 °C in solution 1 (2% potassium acetate, 0.8% sorbitol, 10 mM dithiothreitol, 130 mg ml^{-1} zymolyase 100T (Seikagaku)). Solution 2 (100 mM MES (pH 6.4), 1 mM EDTA, 0.5 mM $MgCl_2$, 1 M sorbitol) was added to stop spheroplasting. Spheroplasted cells (15 μl) were fixed with 30 μl of fixative solution (4% paraformaldehyde, 3.4% sucrose) and lysed with 60 μl 1% lipsol. After addition of 60 μl fixative solution, cells were spread using a glass rod. After drying, the slides were blocked in blocking buffer (0.2% gelatine, 0.5% BSA in PBS) and stained with the following antibodies: anti-HA (3F10, 1:500 dilution, Roche), and anti-Nop1 (1:500 dilution, Encor Biotechnology).

CHEF gel electrophoresis and Southern blotting. Chromosome fragments for CHEF analysis were prepared by restriction digest in agarose plugs. Briefly, 20 ml of meiotic cells were killed by addition of sodium azide (0.1% final w/v), pelleted and stored on ice for the duration of the time course. Cell pellets were washed twice in CHEF-TE (10 mM Tris-HCl (pH 7.5), 50 mM EDTA) and resuspended in 300 μl CHEF-TE. Tubes were individually treated as follows: 4 μl zymolyase T100 (10 mg ml^{-1}) was added and the mix was incubated at 42 °C for 30 s before addition of 500 μl low-melting-point agarose (1.5% SeaPlaque GTG, 125 mM EDTA) at 42 °C. Gel plugs (90 μl) were allowed to harden on ice in disposable plug molds (Bio-Rad) and incubated overnight at 37 °C in 300 μl LET (10 mM Tris (pH 7.5), 500 mM EDTA) per plug. Plugs were deproteinized overnight at 50 °C in 200 μl NDS-PK (LET, 1% *N*-lauroylsarcosine, 1 mg ml^{-1} proteinase K (Amresco)) per plug. Proteinase K was inactivated by incubating plugs for 1 h at 4 °C in CHEF-TE containing 1 mM PMSF, and plugs were washed three times in CHEF-TE, then digested with XhoI in digestion buffer containing 5 mM spermidine. To analyse the entire rDNA array, digested chromosomes were separated by CHEF gel electrophoresis in 1% agarose in 0.5× TBE, 6 V cm^{-1}, using 60-s pulses for 15 h and 90-s pulses for 9 h. For fine mapping of rDNA insertions and to analyse changes in repeat number, digested chromosome fragments were separated using a 5–20 s ramp over 20 h. For conventional electrophoresis, DNA fragments were separated on 0.6% agarose in 1× TBE and transferred onto Hybond-XL membranes (GE Healthcare) by alkaline transfer. Southern blotting was performed as previously described[32] and quantified with a Fujifilm BAS-2500 image reader V1.8 and Multi Gauge V2.2 software.

Probes for Southern analysis. Probe templates for non-rDNA sequences were generated by nested PCR and gel purification. The following probes (SGD coordinates) were used:

YLR164W: XII, 493,432–493,932.
YCR047C: III, 209,361–210,030.
ARS1216: XII, 450,407–451,150.
YLR152C: XII, 443,849–444,910.
NTS1: XhoI and XbaI digest of pRS306-NTS1/2. This probe detects all *NTS1* and *NTS2* sequences (pan-rDNA probe).

rDNA insertion: BciVI digest of pRS306-NTS1/2. This probe specifically detects the plasmid backbone of the *URA3* insertion cassette.
TOM1/*YDR457W*: IV: 1,370,714–1,371,733

Flow cytometry. At the indicated time points, 150 µl of meiotic cells were fixed for 2 h at 4 °C after addition of 350 µl absolute ethanol. Cells were resuspended in 500 µl of 50 mM sodium citrate containing 0.7 µl RNase A (30 mg ml^{-1}, Sigma). Cells were incubated for 2 h at 50 °C. 10 µl proteinase K (Amresco) was added and cells were deproteinated for 2 h at 50 °C. 500 µl of 50 mM sodium citrate containing 0.2 µl Sytox Green (Amersham) was added to the cells. Cells were briefly sonicated and analysed using a FACScalibur (Becton Dickinson) flow cytometer. DNA profiles were generated using CellQuest software.

Recombination mapping. To determine crossover recombination rates, cells were sporulated for 24 h in 3 ml SPO and treated with zymolyase (1 mg ml^{-1} in 1 M sorbitol) to remove ascus walls. Tetrads were dissected by micromanipulation and marker segregation was determined by replica plating on appropriate selective media. For mapping within the rDNA, only tetratypes were used to calculate recombination rates, to avoid distortions originating from non-parental ditypes that were probably the result of previous mitotic recombination.

24. Bell, S. P. *et al.* The multidomain structure of Orc1p reveals similarity to regulators of DNA replication and transcriptional silencing. *Cell* **83,** 563–568 (1995).
25. Kobayashi, T. Strategies to maintain the stability of the ribosomal RNA gene repeats—collaboration of recombination, cohesion, and condensation. *Genes Genet. Syst.* **81,** 155–161 (2006).
26. Chernoff, Y. O., Vincent, A. & Liebman, S. W. Mutations in eukaryotic 18S ribosomal RNA affect translational fidelity and resistance to aminoglycoside antibiotics. *EMBO J.* **13,** 906–913 (1994).
27. Peoples, T. L. *et al.* Close, stable homolog juxtaposition during meiosis in budding yeast is dependent on meiotic recombination, occurs independently of synapsis, and is distinct from DSB-independent pairing contacts. *Genes Dev.* **16,** 1682–1695 (2002).
28. James, P., Halladay, J. & Craig, E. A. Genomic libraries and a host strain designed for highly efficient two-hybrid selection in yeast. *Genetics* **144,** 1425–1436 (1996).
29. Blitzblau, H. G. *et al.* Mapping of meiotic single-stranded DNA reveals double-stranded-break hotspots near centromeres and telomeres. *Curr. Biol.* **17,** 2003 (2007).
30. Blitzblau, H. G. & Hochwagen, A. Genome-wide detection of meiotic DNA double-strand break hotspots using single-stranded DNA. *Methods Mol. Biol.* **745,** 47–63 (2011).
31. Loidl, J., Nairz, K. & Klein, F. Meiotic chromosome synapsis in a haploid yeast. *Chromosoma* **100,** 221–228 (1991).
32. Hunter, N. & Kleckner, N. The single-end invasion: an asymmetric intermediate at the double-strand break to double-holliday junction transition of meiotic recombination. *Cell* **106,** 59–70 (2001).